Chemistry–A European Journal
Research Article
doi.org/10.1002/chem.202300757
Chemistry Europe
European Chemical Societies Publishing
www.chemeurj.org

Special Collection

CO_2 Activation on Cu/TiO_2 Nanostructures: Importance of Dual Binding Site

Ilaria Barlocco,[a] Farahnaz Maleki,[a] and Gianfranco Pacchioni*[a]

Abstract: CO_2 adsorption and activation on Cu single atom catalysts and Cu nanoclusters supported on the (110) surface of rutile and on the (101) surface of anatase TiO_2 have been investigated by means of first principles electronic structure calculations. The role of oxide reduction associated to the presence of oxygen vacancies has been considered. Five main messages emerge from this study. (1) CO_2 activation on Cu/TiO_2 nanostructures is surface sensitive, as the rutile and anatase surfaces can exhibit different behaviors; (2) the surface morphology is essential since CO_2 is activated only when the molecule can simultaneously bind to at least two active sites, such as a Cu atom on one side and an oxide ion on the other site; (3) Cu atoms on TiO_2 are in the +I oxidation state and can bind and activate CO_2 via charge transfer from the oxide; (4) on supported Cu clusters CO_2 activation occurs mostly at the metal/oxide interface; (5) the presence of O vacancy sites facilitates the spontaneous dissociation of CO_2 to CO, or increases the electron density of the metal catalyst, two effects that can influence the mechanism of CO_2 reduction to methanol or other chemicals.

Introduction

The reduction of CO_2 to C1 and C2 molecules and hydrocarbons is a central process in the current energy transition.[1,2] The large number of available catalytic pathways leads to multiple products, limiting selectivity.[3] Catalytic CO_2 reduction reactions always start with the adsorption, electron transfer to CO_2, and activation of the molecule.[4] This initial activation step largely determines which metal catalyst shows appreciable activity toward CO_2 reduction.

The next step consists in the addition of an H atom with possible formation of *OCHO (O-bound) and *COOH (C-bound) intermediates.[5,6] The *OCHO reaction can proceed with formation of formic acid, HCOOH, while the *COOH path leads to CO. In some cases H addition leads to the reverse water gas-shift reaction, with dissociation of the C–O bond.[5] More complex is the formation of C2 products where direct C–C bonds are formed and in particular ethanol. Identifying possible catalysts compositions that favor the C2 versus C1 products is an ambitious target of present research in catalysis.

Cu is a material that can catalyze the conversion of CO_2 to C2 products with acceptable efficiencies.[7–9] Some studies report that oxide derived Cu materials are often superior toward CO_2 reduction than pure Cu and that Cu^+ ions and surface or sub-surface oxygen can be responsible for the activity of oxide-derived Cu catalysts.[4] In particular, an important role is that played by the metal-oxide interface in promoting CO_2 activation.[10]

In order to study this problem, we have performed Density Functional Theory (DFT) calculations considering models of nanocatalysts consisting of highly dispersed Cu species supported on titanium dioxide. When metal species are deposited at low concentration on oxide supports, depending on the preparation conditions one can form isolated metal species, often referred to as single atom catalysts, small metal clusters (< 10-20 atoms) or nanoparticles.[11] In practical conditions it is very difficult to obtain monodispersed distributions of metal nanostructures, and usually both single atoms and nanoclusters are present on the surface of real catalysts, with proportions that depend on the amount of metal deposited, annealing temperature, surface morphology, etc.[12]

In this work we have addressed this aspect by considering two extreme models of supported Cu nanocatalysts on titania, a single Cu atom and a small Cu_{10} cluster. These two systems can be considered as representative of rather different situations. In the first one the active species is an isolated metal atom, and the reactivity depends on the coordination, oxidation state, bonding nature, etc.[13] In the second case the small Cu cluster represents some of the complex aspects associated to these systems: metal-metal bonds, metal/oxide interface, low-coordinated metal sites, etc.

Several catalytic reactions are surface sensitive. TiO_2 has two stable polymorphs that are often encountered in real catalytic systems, rutile and anatase (P25, a classical titania photocatalyst, contains more than 70% anatase with a minor amount

[a] Dr. I. Barlocco, Dr. F. Maleki, Prof. Dr. G. Pacchioni
Dipartimento di Scienza dei Materiali
Università di Milano-Bicocca
via Cozzi 55, 20125 Milano (Italy)
E-mail: gianfranco.pacchioni@unimib.it
Homepage: https://qclab.mater.unimib.it/

Supporting information for this article is available on the WWW under https://doi.org/10.1002/chem.202300757

This article is part of a joint Special Collection in honor of Maurizio Prato.

of rutile and a small amount of amorphous phase). Thus, we considered both single Cu atoms and Cu_{10} clusters deposited on the most stable rutile, r-TiO_2(110), and anatase, a-TiO_2(101), surfaces. The Cu/TiO_2 support is of particular interest for CO_2 reduction.[14–17]

The final aspect considered is the role of surface reduction on the catalytic properties of supported Cu nanocatalysts. Titania is a reducible oxide, and it is hardly produced in stoichiometric form. The most common defect is the oxygen vacancy, a defect center that has been widely studied and discussed in the literature.[18] We have considered reduced r-TiO_{2-x}(110) and a-TiO_{2-x}(101) surfaces by creating O vacancies in various positions and we studied the effect of the reduction on the catalytic activity of the Cu nanostructures in CO_2 activation.

From this systematic analysis we derive some general notions about the potential role of highly dispersed Cu-based species on titania in the activation of CO_2. This is an essential prerequisite for the further study of possible reaction steps in the thermal, photocatalytic or electrocatalytic reduction to CO_2 to C1 or C2 products.

The paper is organized as follows. After a description of the computational method adopted, we discuss the nature and the properties of isolated Cu atoms stabilized on rutile and anatase and their capability to stably bind carbon dioxide. Both stoichiometric and reduced surfaces are discussed. In Section 3.2 the same problem is analyzed but now for the case of a supported Cu_{10} cluster. The Conclusions summarize the results and in particular: (1) the process is surface sensitive; (2) the presence of double binding sites is essential for CO_2 activation; (3) single Cu atoms on TiO_2 can activate CO_2 via direct charge transfer; (4) there is special reactivity of the Cu and O atoms at the Cu cluster/oxide interface; (5) oxide reduction can play an important role provided that the O vacancies are in direct contact with the Cu catalyst.

Results and Discussion

CO_2 adsorption on Cu_1/TiO_2

Rutile and anatase stoichiometric surfaces: Cu_1/TiO_2

In this section, we discuss the activation of CO_2 by an isolated Cu atom adsorbed on the rutile (110), r-TiO_2, and anatase (101), a-TiO_2, surfaces. Single atom catalysts can assume various positions on oxide surfaces, and recent studies have shown the important role of surface O atoms and OH groups in stabilizing the atomic species.[19,20] In some cases, however, it has been shown that the metal atoms can be simply bound to the surface

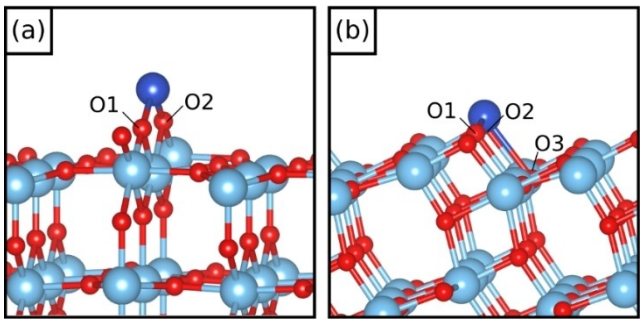

Figure 1. Most stable isomers of Cu single atom adsorbed on a) r-TiO_2 and b) a-TiO_2. Red: oxygen; light blue: Ti; dark blue: Cu.

in a stable adsorption site, as for Rh atoms on the anatase (101) surface.[21] Here we considered various non-equivalent adsorption sites on the two different supports, as also discussed in the literature,[22–25] see Section S1 and Figure 1. The Cu atom interacts in a similar way with the two TiO_2 surfaces, Table 1. In fact, on both rutile and anatase, Cu bridges two O_{2c} atoms on the surface, with similar adsorption energies, $E_{ads} = -2.19$ eV (rutile) and $E_{ads} = -2.31$ eV (anatase), and Cu–O bond distances, about 1.9 Å. In both cases we observe a net positive Bader charge on the Cu atom, $+0.71\ |e|$ for r-TiO_2 and $+0.66\ |e|$ for a-TiO_2, indicating a transfer of one electron from Cu to the support. In principle this charge transfer should be visible also from the analysis of the spin density. In fact, in the case of r-TiO_2 a spin density close to 1 is found with the unpaired electron localized over the Ti atoms of the support. The spin polarization is not found for a-TiO_2 as the charge transferred is completely delocalized over the TiO_2 conduction band. This problem is well known and is related to the formation of polarons and their description in DFT.[26] The formation of a polaron depends on the kind of exchange-correlation functional used, as self-interaction corrected functionals are required to see this phenomenon.[27] However, polaron formation is not essential for our discussion and is outside the scope of the present study.

Rutile and anatase reduced surfaces: Cu_1/TiO_{2-x}

We have seen above that on stoichiometric titania surfaces a Cu atom is expected to be in a positive oxidation state. In principle, the activation of CO_2 should become more favorable by increasing the electron density on Cu,[28] an effect that could be obtained if Cu is bound to electron-rich centers such as the oxygen vacancies. In fact, oxygen vacancies in titania result in

Table 1. Adsorption energy (E_{ads}), Bader charge of Cu ($|q|$), Cu–O bond distances (R) and spin density for the most stable isomers of a Cu single atom adsorbed on the r-TiO_2 and a-TiO_2 surfaces.

Structure	E_{ads} [eV]	q(Cu) [$\|e\|$]	R_{Cu-O} [Å] Cu–O1	Cu–O2	Cu–O3	spin
Cu/r-TiO_2	-2.19	0.71	1.87	1.87	–	1
Cu/a-TiO_2	-2.31	0.66	1.89	1.89	2.43	0

excess electrons that localize on the Ti 3d states, with Ti ions that change their oxidation state from +IV to +III.[27,29] The presence of O vacancies can alter the charge state of the active phase.[30] We created models of reduced r-TiO_{2-x} and a-TiO_{2-x} by removing O atoms from the surface or sub-surface layers, see Figure 2 and Table S2.1. The formation energy and relative stability of O vacancies in TiO_2 have been studied in detail in the past, and the results are partly method dependent.[31]

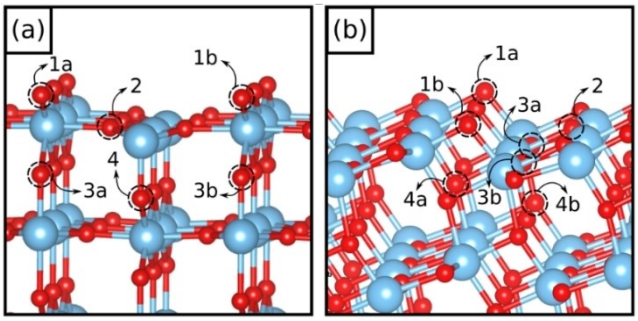

Figure 2. O atoms that have been removed to create models of (a) reduced r-TiO_2 and (b) reduced a-TiO_2. Red: oxygen; light blue: Ti; dark blue: Cu.

Table 2. Adsorption energy (E_{ads}), Bader charge of Cu (q), Cu–O bond distance (R) and spin density of various isomers of Cu single atom adsorption on r-TiO_2 and a-TiO_2 reduced surfaces.

Figure 3	Vac. type	E_{ads} [eV]	q(Cu) [|e|]	R_{Cu-O} [Å]	spin
(a)	O1	−2.04	0.70	1.86/1.86	1
(b)	O3	−1.72	0.70	1.87/1.87	2
(c)	O1	−1.46	−0.24	3.05/3.05	1
(d)	O1a	−2.40	−0.03	2.20/2.34/2.46	0
(e)	O4b	−2.37	0.63	1.87/1.87	0
(f)	O4a	−2.21	0.65	1.88/1.88/2.47	0

On the surface layer of both rutile and anatase the lowest vacancy formation energy (E_f) is obtained by removing an O_{2c} atom: E_f-O1(r-TiO_{2-x}) = 3.05 eV and E_f-O1(a-TiO_{2-x}) = 4.70 eV. Considering the sub-surface layer, the most favorable structure was obtained by removing O3 in case of rutile and O4 in anatase, see Figure 2, with E_f-O3(r-TiO_{2-x}) = 3.74 eV and E_f-O4(a-TiO_{2-x}) = 5.18 eV. This latter result contrasts with the experimental evidence that on anatase it is preferred to form sub-surface vacancies;[32,33] the discrepancy is due to the DFT + U approach used here. On the other hand, the use of DFT + U guarantees a better description of the titania band gap. This is essential in order to avoid the risk to find unphysical charge transfers from the adsorbate (Cu in this case) and the oxide support due to an energetically too low conduction band edge.

On the variously reduced r-TiO_{2-x} and a-TiO_{2-x} surfaces we have adsorbed a Cu atom, Table 2, Figure 3 and also Section S2 in the Supporting Information.

Starting from Cu/r-TiO_{2-x}, one can observe different features depending on the type of vacancy created, but in general the binding energy of the Cu atom to the surface decreases slightly compared to stoichiometric surface (E_{ads} = −2.04 eV, reduced, Table 2, compared to E_{ads} = −2.14 eV, stoichiometric, Table 1). Indeed, in the most stable structure, Figure 3(a), the Cu coordination, adsorption energy and Bader charge do not change significantly compared to the stoichiometric Cu/r-TiO_2 case. This is not too surprising if we consider that the Cu atom and the O vacancy are in two parallel rows of O_{2c} atoms, Figure 3(a), so that their mutual interaction is negligible. Even the charge on the adsorbed Cu atom is the same on the reduced and stoichiometric surface, about +0.7 |e|.

A similar coordination and Bader charge was found also in the second most stable structure, Figure 3(b), where a sub-surface O-vacancy is present but far from the adsorbed Cu

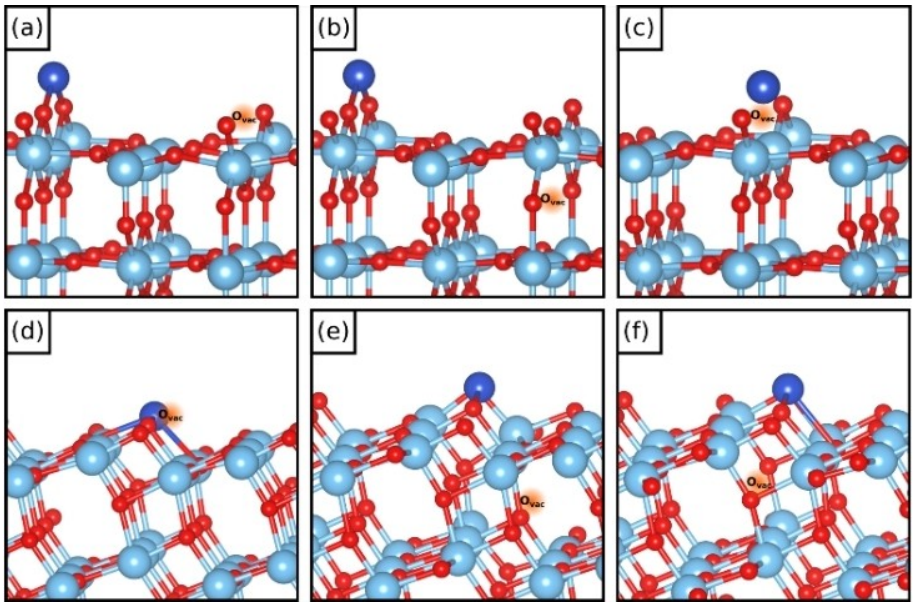

Figure 3. Most stable isomers of Cu single atom adsorption on a)–c) r-TiO_{2-x} and d)-f) a-TiO_{2-x} surfaces with one O vacancy. Red: oxygen; light blue: Ti; dark blue: Cu.

atom. However, in this case E_{ads}(Cu) is significantly lower than in previous case, by about 0.5 eV. More dramatic is the change observed for the third system, Figure 3(c), where the change in E_{ads} going from the stoichiometric to the reduced surface is 0.73 eV. Here, the Cu atom is directly bound on an O vacancy created by removing the O_{2c} site, so that Cu interacts directly with a Ti_{4c} and a Ti_{5c} sites ($R_{Ti\text{-}Cu}$ = 2.58 Å). In this case, we observe a clear charge transfer from the oxide support to the metal atom, as shown by Bader charge: q(Cu) = −0.24 |e|, Table 2. The weaker interaction of the Cu atom with an O vacancy than with the regular surface is a bit surprising since in general O vacancies are trapping sites for adsorbed metal species and bind more strongly than non-defective sites.[34] But the case of Cu is somewhat special due to the tendency of this atom to transfer electrons to the support, an effect that is not favored by the presence of a reduced surface where excess electrons are already present.

The situation is completely different when we consider the anatase (101) surface. On Cu/a-TiO_{2-x} the most stable isomer corresponds to a Cu atom directly bound to a surface O vacancy, Figure 3(d). The metal binds to two O_{3c} and one O_{2c} atoms, giving an E_{ads} slightly higher, in absolute value, than that found on the stoichiometric system: ΔE_{ads} (reduced-stoichiometric) = −0.09 eV. An increased electron density is found on Cu as shown by the Bader charge, q(Cu) = −0.03 |e|. One of the two excess electrons associated to the O vacancy in the unit cell is transferred to the Cu atom that from positively charged (stoichiometric surface) becomes charge neutral.

We also considered cases where Cu is adsorbed on a-TiO_2(101) in the presence of sub-surface O vacancies, see Figures 3(d) and (e). Here the adsorption characteristics are very similar to those of the regular surface, showing that there is no indirect interaction between the O vacancies and the Cu adatom, see Table 2.

From these results it turns out that only if the Cu atom is directly bond to an O vacancy its electron density increases and its charge state becomes neutral or slightly negative. In all other cases the atom is in a +I oxidation state.

We checked that this result is independent of the concentration of O vacancies. We created a second O_{vac} center in the supercell to increase the excess of the electronic charge in the support, but we found that this has a negligible effect on the electron density and coordination mode of the Cu species. For further info see section S3 in the Supporting Information.

CO adsorption on Cu_1/TiO_2 and Cu_1/TiO_{2-x}

An approach that can provide useful information on the charge state of supported transition metal (TM) atoms is to use CO as a probe molecule.[35,36] One can measure (and compute) the vibrational properties and in particular the C–O stretching mode of the TM-CO complexes. CO in fact is a molecule with moderate reactivity and is very sensitive to the electronic nature of the adsorption site.[37] Thus, we computed the vibrational modes of adsorbed CO using the harmonic approximation for two representative situations: CO adsorbed on a Cu atom bound to the stoichiometric titania surfaces, Cu/TiO_2, see Figures 4(a) and (c) and Table 3, and CO adsorbed on Cu atoms stabilized on reduced titania, Cu/r-TiO_{2-x} and Cu/a-TiO_{2-x}. In this latter case we considered a O_{2c} vacancy created near the Cu atom, see Figure 4(b, d).

When Cu is adsorbed on the stoichiometric surfaces, the CO–Cu bond has similar characteristics on rutile and anatase: the CO–Cu binding energy is about 1 eV, and the CO vibrational frequency is blue-shifted by +54 cm^{-1} for rutile and by +3 cm^{-1} for anatase. The presence of a blue-shift is fully consistent with a positive oxidation state of the Cu atom. Completely different is the situation on the reduced surfaces,

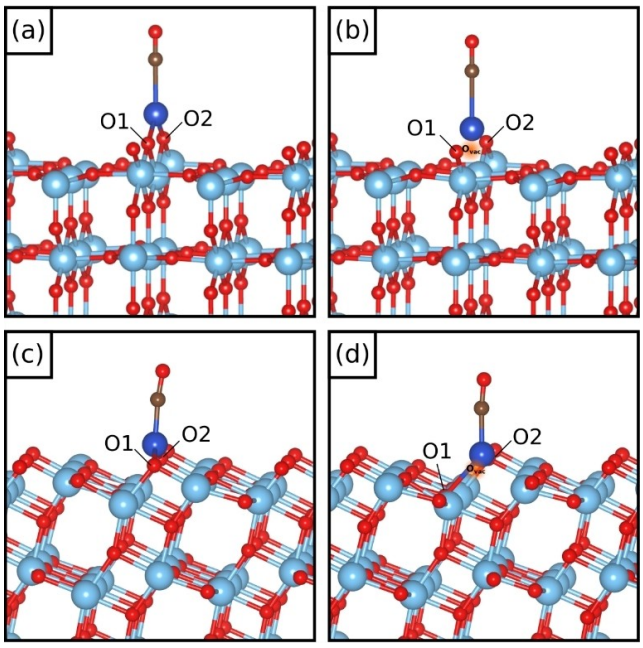

Figure 4. CO molecule adsorption on (a) Cu/r-TiO_2, (b) Cu/r-TiO_{2-x}, (c) Cu/a-TiO_2 and (d) Cu/a-TiO_{2-x}. Red: oxygen; light blue: Ti; dark blue: Cu.

Table 3. Adsorption energy (E_{ads}), CO stretching frequency (ν), Bader charges (q), bond distances (R) for CO molecule adsorption on (a) Cu/r-TiO_2, (b) Cu/r-TiO_{2-x}, (c) Cu/a-TiO_2 and (d) Cu/a-TiO_{2-x}.

Figure 4	E_{ads} (CO) [eV]	ν [cm^{-1}]		q [|e|]		R [Å]			
		ν_{CO}	$\Delta\nu_{CO}$	Cu	CO	Cu–O1	Cu–O2	Cu–C	C–O
(a)	−1.05	2177	54	0.76	−0.02	1.89	1.89	2.26	1.13
(b)	−0.11	1621	−502	−0.17	0.01	3.05	3.05	2.39	1.21
(c)	−1.08	2126	3	0.75	−0.05	2.01	2.00	1.79	1.15
(d)	−1.00	2098	−25	0.16	−0.09	2.32	2.33	1.83	1.15

which reflects also the different Cu charge state. On reduced rutile, Cu/r-TiO_{2-x}, CO is very weakly bound, −0.11 eV, and the C–O stretching mode is enormously red-shifted, by −502 cm^{-1}. This is consistent with a negatively charged Cu atom, but the very weak binding energy also suggests that CO will not bind to Cu/r-TiO_{2-x} at temperatures above about 50 K.

On reduced anatase, Cu/a-TiO_{2-x}, the CO–Cu binding energy is about 1 eV, and the C–O stretching frequency is slightly red-shifted by −25 cm^{-1}. This is consistent with a neutral Cu atom as shown by the Bader charge. Thus, also in this case the calculation of the CO stretching frequency confirms the results deduced from the analysis of the Bader charges.

CO_2 adsorption on Cu_1/TiO_2 and Cu_1/TiO_{2-x}

Previous studies from the literature have shown that the rutile clean surface interacts only weekly with CO_2.[38,39] Indeed, also our calculations show that the CO_2 molecule is only physisorbed on the rutile surface, retaining its initial conformation, i.e. $\widehat{OCO}$ = 178.3°, R_{C-O} = 1.18 Å and R_{Ti-O} = 2.82 Å.

The presence of an isolated Cu atom changes the scenario. In fact, CO_2 is activated at the interface between the Cu single atom and the rutile surface, binding to two Ti_{5c} ions with the O atoms and to the Cu atom with C, see Figure 5(a). In this configuration, the molecule is bent, $\widehat{OCO}$ = 129.4°, and the C–O bonds are elongated, R_{C-O} = 1.27 Å, Table 4, compared to the gas-phase molecule. In this configuration the CO_2 molecule is bound to the catalyst by −0.42 eV, which is indicative of the formation of a true chemical bond of medium strength.

The activation of CO_2 in this structure is due to the fact that the molecule becomes negatively charged, q(CO_2) = −0.73 |e|, Table 4. However, the Bader charge on Cu, q(Cu) = +0.73 |e|, is the same found in absence of CO_2, see Table 1, showing that the Cu atom is still in a +I oxidation state. In fact, the excess electron transferred from Cu to r-TiO_2 remains localized on a Ti *3d* orbital (see Supporting Information). Therefore, charge flows from the oxide surface to the adsorbed CO_2 molecule without modifying the charge state of the Cu atom. On the other hand, the Cu atom is essential for the process, as it provides an additional binding site for CO_2, Figure 5(a). The presence of this conformation and of a multiple binding site is key to the entire activation process.

Next, we considered the same process but in the presence of an O vacancy. The vacancy has been placed in various surface and sub-surface positions, see Figures 5(b–d). In the three cases considered, the CO_2 molecule is always strongly bound, from −0.84 eV to −1.54 eV, Table 4, and activated, as shown by the $\widehat{OCO}$ angle that is close to 120°, and by the elongated C–O bonds.

The origin of the strong activation on the reduced Cu/TiO_{2-x} support becomes clear if one looks at the Bader charges, Table 4, and at spin distribution, Figure S5.2. The Bader charge on Cu, q(Cu) = +0.5/+0.7 |e|, is the same found in absence of CO_2, see Table 1. The net charge on the CO_2 adsorbate, however, q(CO_2) = −1.0 |e|, Table 4, and the spin distribution, Figure S5.2, clearly show that a full electron has been transferred to the CO_2 unit. This is due to the fact that the presence of an O vacancy results in two excess electrons on the rutile support; a third electron is donated by the Cu atom. The reduced surface is thus electron-rich, and the Cu/TiO_{2-x} Fermi level moves up in energy. When CO_2 binds to the Cu catalyst part of the excess of electronic charge is transferred back, leading to a substantial activation of the adsorbed CO_2 molecule.

For both stoichiometric, Cu/r-TiO_2, and reduced, Cu/r-TiO_{2-x}, systems the activation of CO_2 is strongly favored by the rutile

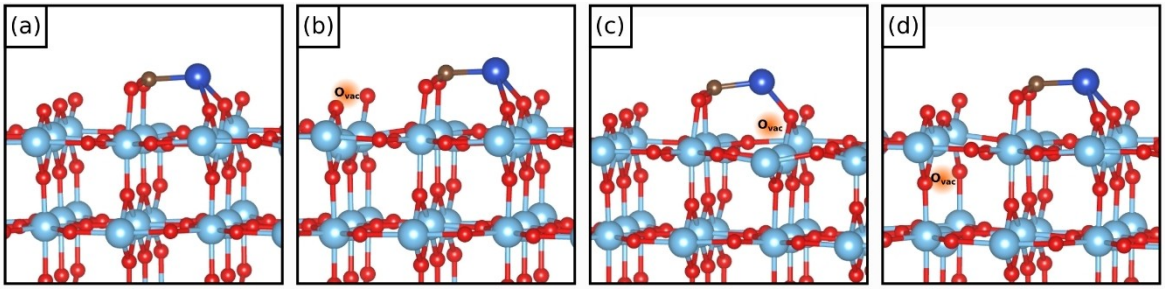

Figure 5. CO_2 molecule adsorption on (a) Cu/r-TiO_2 and (b–d) Cu/r-TiO_{2-x}. Red: oxygen; light blue: Ti; dark blue: Cu.

Table 4. Adsorption energy (E_{ads}), Bader charge (*q*), bond distances (*R*), CO_2 bond angle (∠OCO) and total spin density for various isomers of CO_2 adsorption on Cu/r-TiO_2 and Cu/r-TiO_{2-x}.

Figure 5	Vac.	E_{ads} [eV]	*q* [|e|] Cu	CO_2	*R* [Å] Cu–O	Cu–C	Ti–O	C–O	∠OCO [°]	spin
(a)	–	−0.42	0.73	−0.73	2.01/2.01	1.92	2.15/2.15	1.27/1.27	129.4	1
(b)	O1	−0.84	0.67	−1.05	2.074/2.074	1.88	1.96/1.98	1.31/1.31	117.2	1
(c)	O1	−1.54	0.55	−1.04	1.87	1.86	1.97/2.02	1.29/1.32	118.6	1
(d)	O3	−1.26	0.70	−1.07	2.07/2.08	1.88	1.97/1.97	1.31/1.31	116.9	1

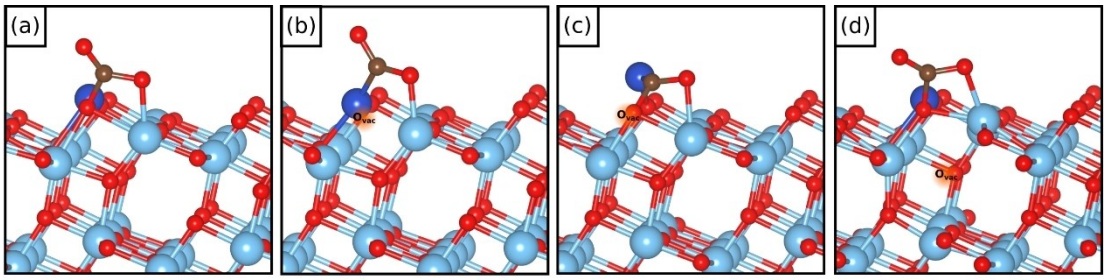

Figure 6. CO_2 molecule adsorption on (a) Cu/a-TiO_2 and (b–d) Cu/a-TiO_{2-x}. Red: oxygen; light blue: Ti; dark blue: Cu.

(110) surface morphology that allows an optimal interaction of the molecule with two Ti_{5c} atoms on one side, and the Cu atom on the other side, Figure 5. As we mentioned above, the possibility to form multiple bonds and to coordinate to more than one active site is essential for the formation of a stable activated CO_2 complex.

Now we consider the anatase surface where things change substantially. The first difference lies in the reactivity of the two bare surfaces towards CO_2. We have seen above that on r-TiO_2(110) CO_2 is only weakly physiosorbed, in agreement with previous studies.[38,39] On the (101) anatase surface, on the contrary, CO_2 binds with an O_{2c} atom of the surface via C, and with a Ti_{5c} atom via O, resulting in a small $E_{ads} = -0.25$ eV, Figure S5.1, and significant activation, as shown by the $\widehat{OCO}$ angle, 131.1°, and the C–O bonds, elongated to 1.20 Å and 1.31 Å, respectively. This result agrees with previous accurate studies on the same system.[40]

Next, we tried to adsorb the CO_2 molecule on the Cu/a-TiO_2(101) stoichiometric surface, in analogy with the rutile case. However, starting the geometry optimization with CO_2 bound to Cu, we found that the minimum structure corresponds to the same structure described before, where CO_2 interacts only with the anatase surface: the Cu adatom is only a spectator species, Figure 6(a). This reflects in similar geometrical parameters of adsorbed CO_2 with and without Cu atom (see Table 5 and Figure S5.1). Even the binding energies are similar and close to zero, indicating that it is very unlikely that an isolated Cu atom on the regular anatase surface will stably bind and activate a CO_2 molecule.

On the reduced anatase surface, Figures 6(b–d) the situation looks more similar to what we have seen in the case of reduced rutile. In the presence of a O_{2c} surface vacancy, Figure 6(b), the Cu atom has enough electron density to strongly interact with CO_2, see $E_{ads} = -1.42$ eV. The most stable structure, however, ($E_{ads} = -1.85$ eV) is obtained when an O atom of CO_2 fills the cavity left by the removed O_{2c} atom, Figure 6(c), thus displacing the Cu atom from its original position. In both activated structures the $\widehat{OCO}$ angle is 110–130° and the CO_2 molecule carries a substantial negative charge while the Cu atom remains in a positive oxidation state, as for reduced rutile TiO_2.

The importance of a direct contact of the Cu atom with a surface O vacancy is demonstrated by the last case discussed here, Figure 6(d), where a sub-surface O vacancy has been created. In this case, in fact, CO_2 interacts with the Cu atom in a similar fashion as on the non-defective Cu/a-TiO_2 support, exhibiting a small and positive $E_{ads} = +0.20$ eV (unbound complex) and an almost neutral CO_2 adsorbate, see Table 5. This shows that only when the O vacancies are present on the surface of anatase they have a marked effect on CO_2 activation on Cu/a-TiO_{2-x} single atom catalysts.

CO_2 adsorption on Cu_{10}/TiO_2

Cu_{10} cluster on stoichiometric TiO_2 surfaces

In order to study CO_2 activation on supported Cu nanostructures, a Cu_{10} cluster was adsorbed on the bare anatase and rutile surfaces forming Cu_{10}/r-TiO_2(110) and Cu_{10}/a-TiO_2(101) model catalysts, respectively. We selected as initial conformation of the Cu_{10} cluster a structure formed by two layers containing seven Cu atoms in the bottom layer (in contact with the support) and three Cu atoms in the top layer. In this way, both Cu atoms coordinated to the oxide surface and Cu atoms bound only to other Cu atoms are present in the model which has been successfully used for other studies of supported metal

Table 5. Adsorption energy (E_{ads}), Bader charge (q), bond distances (R), CO_2 bond angle (∠OCO) and spin density for various isomers of CO_2 adsorption on Cu/a-TiO_2 and Cu/a-TiO_{2-x}.

Figure 6	Vac.	E_{ads} [eV]	q [|e|] Cu	CO_2	R [Å] C–O1	Cu–C	Ti–O	C–O	∠OCO [°]	spin
(a)	–	0.02	0.67	−0.15	1.46	2.75	2.00	1.20/1.31	132.6	0
(b)	O1	−1.42	0.39	−0.77	-	1.91	1.96	1.22/1.32	128.1	0
(c)	O1	−1.85	0.55	−1.16	–	1.84	2.09/2.07/2.17	1.35/1.29	109.4	0
(d)	O4a	0.20	0.66	−0.24	1.50	2.84	2.05	1.20/1.30	135.5	0

clusters,[41] Figure 7. Of course, metal clusters can exist in an enormous number of shapes and conformations, with important consequences on the chemical activity.[42] However, the search of the global minimum for the structure of Cu_{10} is out of the scope of this work. The aim is to compare, on the same footing, a Cu single atom catalyst with one of the many possible structures of Cu nanoclusters supported on the same surface. While the details of the results will certainly depend on the nature of the Cu cluster used to model the nanocatalyst, we believe that the general message will not be affected by this choice.

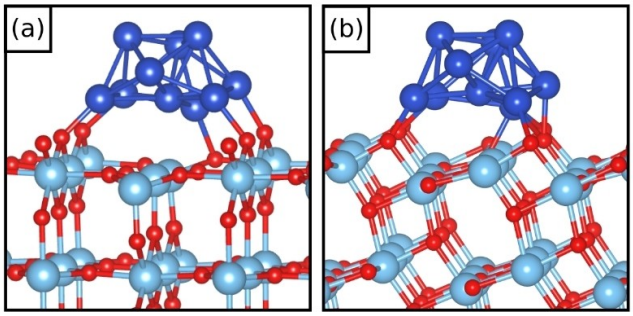

Figure 7. Optimal structure of a Cu_{10} cluster on (a) rutile (110) and (b) anatase (101) TiO_2 surfaces. Red: oxygen; light blue: Ti; dark blue: Cu.

We first optimized the Cu(7,3) cluster in the gas-phase, we deposited it on the r-TiO_2(110) and a-TiO_2(101) surfaces, where it has been fully reoptimized, Figure 7. Cu_{10} interacts with the rutile and anatase surfaces with an adsorption energy of −6.89 eV and −4.72 eV, respectively. The much larger adhesion energy on rutile can be traced back to the good interaction of the basal Cu atoms with the protruding O_{2c} atoms of two adjacent rows. The Bader charge analysis indicates a transfer of electrons from the Cu cluster to TiO_2, resulting in an overall $q(Cu_{10}) = +1.43\ |e|$ for Cu_{10}/r-TiO_2 and $q(Cu_{10}) = +1.41\ |e|$ for Cu_{10}/a-TiO_2, in agreement with our previous study.[41] These two structures have been used to check the reactivity towards CO_2.

CO_2 was adsorbed on various non-equivalent sites in the cluster top and bottom layers, or at the metal/oxide interface, a region of particular interest since recent studies have shown the different reactivity of the periphery of supported metal clusters.[43,44] Previous studies from the literature have shown that the Cu(111) surface is not able to transfer electrons to CO_2.[14,45,46]

The results of the adsorption of CO_2 on Cu_{10}/r-TiO_2(110) are shown in Figure 8 and Table 6 where the corresponding structures are reported in order of decreasing stability. How-

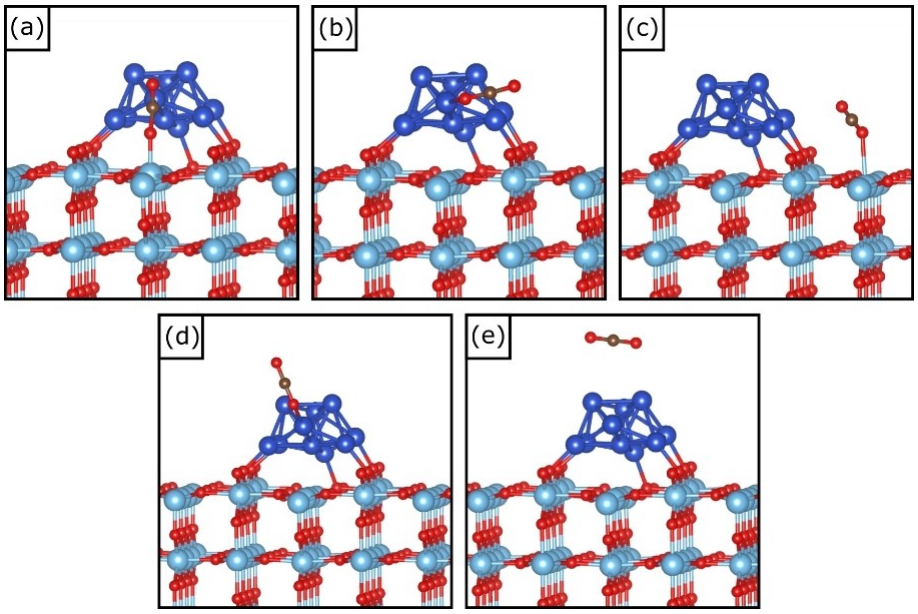

Figure 8. Structure of various isomers of CO_2 adsorption on Cu_{10}/r-TiO_2. Red: oxygen; light blue: Ti; dark blue: Cu.

Table 6. Adsorption energy (E_{ads}), Bader charge (q), bond distances (R), CO_2 bond angle (∠OCO) and spin density for various isomers of CO_2 adsorption on a supported Cu_{10} cluster on rutile.

Figure 8	E_{ads} [eV]	q [|e|]		R [Å]				∠OCO [°]	spin
		Cu_{10}	CO_2	Cu–O	Cu–C	Ti–O	C–O		
(a)	−0.65	1.71	−0.74	–	1.93	1.92	1.30/1.23	126.5	1
(b)	−0.44	1.56	−0.12	2.31	–	–	1.19/1.17	177.3	2
(c)	−0.44	1.50	−0.04	-	–	2.58	1.18/1.17	178.1	2
(d)	−0.38	1.48	−0.01	2.23	–	–	1.18/1.17	179.6	2
(e)	−0.15	1.42	−0.05	3.00/3.32	–	–	1.18/1.18	179.2	2

ever, only in one case we found that CO_2 is activated thanks to the interaction of the C atom with a Cu atom of the cluster and of O with a Ti_{5c} atom of the surface, Figure 8(a). The adsorption energy is $E_{ads} = -0.65$ eV, and the distortion is apparent, $\widehat{OCO}$ angle of 126.5°. For all other structures considered, the CO_2 molecule is virtually unbound, and non-activated, see the $\widehat{OCO}$ angle close to 180°, Table 6 and Figures 8(b–e). The peculiarity of the bound structure, Figure 8(a), lies in the possibility for CO_2 to bind to two sites, as observed also for the Cu atom case.

Once more, important differences are found when the same process is studied using anatase as a support, Figure 9 and Table 7. In the most stable complex, Figure 9(a), CO_2 is strongly bound, $E_{ads} = -1.66$ eV, and CO_2 clearly activated with an $\widehat{OCO} = 119.4°$ and $R_{C-O} = 1.30$ Å. The C atom is bound to a Cu atom from the cluster, in a similar fashion to the case of Cu_{10}/r-TiO_2(110), but on anatase both O atoms of CO_2 interact with Ti_{5c} atoms of the surface. The molecule carries a negative charge of -1.09 |e|. Differently from rutile, other structures have been identified where CO_2 is activated, $\widehat{OCO}$ around 125°, by bonding at the interface of Cu_{10}/a-TiO_2(101). The common denominator of these structures is that CO_2 is activated by bonding simultaneously to Cu atoms and O or Ti atoms of the surface, see Figures 9(b) and (e) and Table 7.

The remaining two structures, Figures 9(c) and (d) are reported for completeness since they exhibit a non-activated linear CO_2 molecule moderately bound to the anatase surface, Figure 9(c), or to the Cu cluster, Figure 9(d). The absence of multiple coordination of the CO_2 molecule results in absence of charge transfer and thus lack of activation.

Cu_{10} cluster on reduced TiO_2 surfaces

In this section we consider the same Cu_{10} cluster discussed above, but this time with an O vacancy created at the interface between the cluster and the support, Figure 10 (rutile) and 11 (anatase). This is justified by several studies that show that the reducibility of oxide surfaces is more pronounced at the metal/oxide interface, as the O atoms in contact with a supported metal particle are easier to remove.[47]

In the case of Cu_{10}/r-TiO_{2-x}(110), the effect of the reduction is quite dramatic. In fact, in all three cases considered the CO_2 adsorption energy becomes negative, indicating an exothermic process and a strong interaction, Table 8. This is particularly relevant for the case of Figure 10(a) where CO_2 adsorption

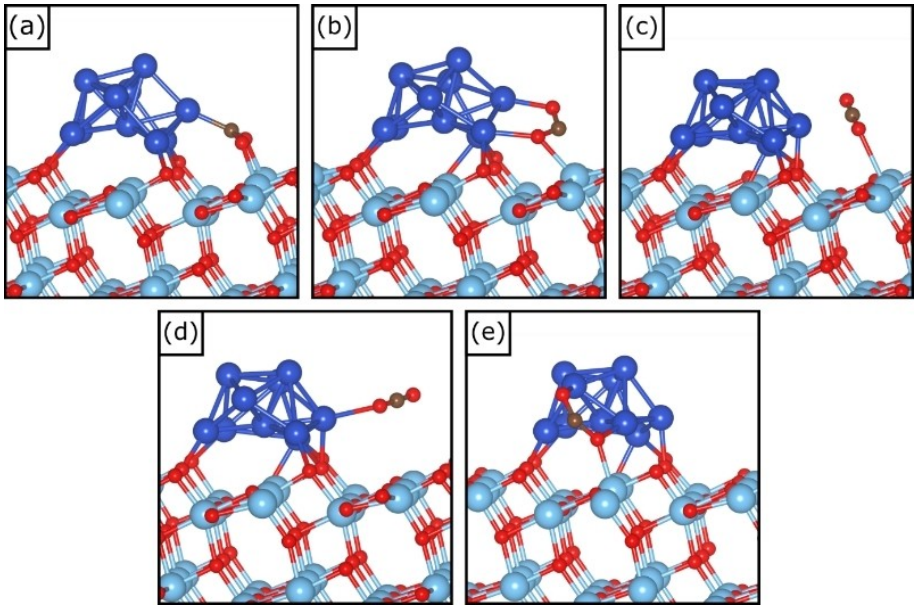

Figure 9. Structure of various isomers of CO_2 adsorption on Cu_{10}/a-TiO_2. Red: oxygen; light blue: Ti; dark blue: Cu.

Table 7. Adsorption energy (E_{ads}), Bader charge (q), bond distances (R), CO_2 bond angle (∠OCO) and spin density for various isomers of CO_2 adsorption on supported a Cu_{10} cluster on anatase.

Figure 9	E_{ads} [eV]	q [|e|] Cu_{10}	CO_2	R [Å] Cu–O	Cu–C	Ti–O	C–O	∠OCO [°]	spin
(a)	−1.66	1.50	−1.09	–	1.94	2.01 2.01	1.30/1.30	119.4	0
(b)	−0.70	1.67	−1.03	2.14/2.00	–	2.17	1.30/1.25	126.2	0
(c)	−0.51	1.50	−0.03	2.95	–	2.63	1.16/1.19	178.0	0
(d)	−0.33	1.46	−0.04	2.32	–	–	1.18/1.17	178.8	0
(e)	−0.12	1.61	−0.83	1.99/2.06	–	2.11	1.24/1.29	124.5	1

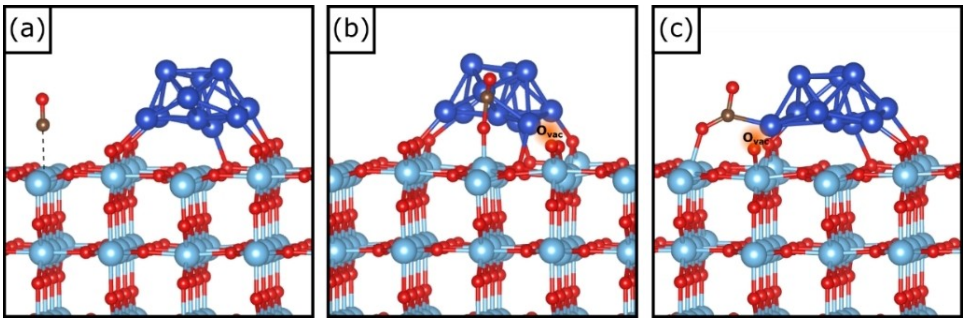

Figure 10. Stable isomers of CO_2 adsorption on Cu_{10}/r-TiO_{2-x}. Red: oxygen; light blue: Ti; dark blue: Cu.

Table 8. Adsorption energy (E_{ads}), Bader charge (q), bond distances (R), CO_2 bond angle (∠OCO) and spin density for various isomers of CO_2 adsorption on Cu_{10}/r-TiO_{2-x}.

Figure 10	E_{ads} [eV]	q [|e|] Cu_{10}	CO_2	R [Å] Cu–C	Ti–O	C–O	∠OCO [°]	spin
(a)	−1.84	1.42	−−	–	–	1.14	–	2
(b)	−1.11	1.38	−0.88	1.92	1.83	1.38/ 1.21	120.5	0
(c)	−0.75	1.20	−0.76	1.96	2.03	1.28/ 1.24	127.1	2

results in the spontaneous dissociation into an O atom that fills the vacancy and an adsorbed CO molecule bound on the rutile surface. E_{ads} in this case is −1.84 eV, which results from the large energy gain associated to the annihilation of the O vacancy, Figure 10(a).

Two less stable structures, Figures 10(b) and (c), are local minima where CO_2 remains intact and strongly bound and activated, as shown by $E_{ads} = -1.11$ eV and $E_{ads} = -0.75$ eV, and $\widehat{OCO}$ angles of about 120°, Table 8. In both cases CO_2 is negatively charged due to the electron transfer from the surface, and is simultaneously interacting with the cluster and the support, similarly to what we observed on the stoichiometric surface (see above). The effect of the excess of charge becomes apparent if one compared the bond strength of CO_2 to Cu_{10}/TiO_2, Figure 8(a) and Table 6, $E_{ads} = -0.65$ eV, with the similar complexes formed in the presence of a vacancy, where E_{ads} decreases by −0.46 eV, see Figure 10(b) and Table 8.

Also in the case of Cu_{10} on the reduced anatase surface, the most stable structure corresponds to the dissociation of the CO_2 molecule, with formation of a CO molecule, this time adsorbed on a Cu atom of the cluster, Figure 11(a), and an O atom that fills the vacancy leading to an overall energy gain of −1.84 eV, Table 9.

In the other systems considered, CO_2 is strongly bound and significantly activated, see in particular the structure shown in Figure 11(b), $E_{ads} = -1.60$ eV and $\widehat{OCO} = 120°$. This structure, however, is similar to the one reported in Figure 9(a) for the stoichiometric anatase surface showing a similar energy of

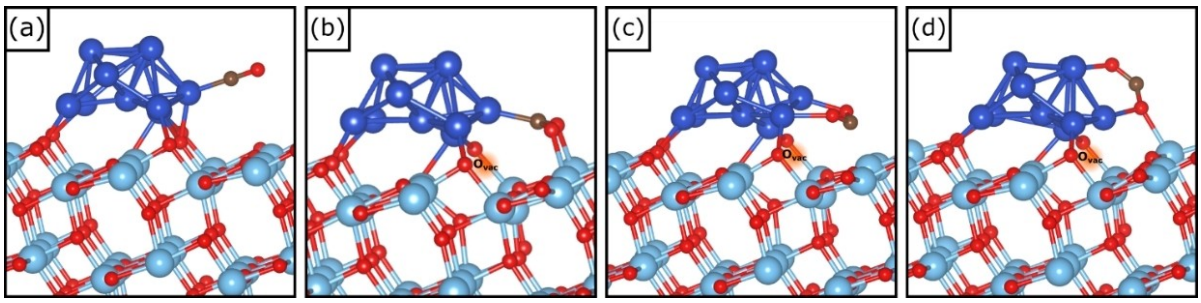

Figure 11. Stable isomers of CO_2 adsorption on Cu_{10}/a-TiO_{2-x}.

Table 9. Adsorption energy (E_{ads}), Bader charge (q), the bond distances (R), CO_2 bond angle (∠OCO) and spin density for various isomers of CO_2 adsorption on Cu_{10}/a-TiO_{2-x}. Red: oxygen; light blue: Ti; dark blue: Cu.

Figure 11	E_{ads} [eV]	q [|e|] Cu_{10}	CO_2	R [Å] Cu–O	Cu–C	Ti–O	C–O	∠OCO [°]	spin
(a)	−1.84	1.51	–	–	1.81	–	1.16	–	0
(b)	−1.60	1.35	−1.09	–	1.90	2.06/2.04	1.29/1.29	120.4	1
(c)	−0.53	1.59	−1.10	2.04/1.95	-	–	1.28/1.28	125.6	1
(d)	−0.19	1.53	−0.75	2.14/2.03	-	2.21	1.28/1.23	129.4	1

adsorption ($\Delta E_{ads} = 0.06$ eV) and an almost identical R_{C-O} and OCO angle, see Table 7 and Table 9. This shows that here the presence of the O vacancy has virtually no effect on the activation of CO_2. A similar comparison can be made between the structures of Figure 11(c) and Figure 9(b) as well as Figure 11(d) and Figure 9(e), indicating that the role of the vacancy is almost negligible when the Cu_{10} cluster is supported on anatase.

Conclusions

Any process of CO_2 conversion to useful chemicals implies an initial step where the molecule is bound to the catalyst and sufficiently activated. The high stability of CO_2 and the weak bonding that usually occurs between the molecule and the catalyst surface represents the first problem encountered in the chemical reduction of CO_2 to C1 or C2 products. The topic has been investigated quite extensively in the past at both fundamental and applied levels,[48,49] with partial understanding of the elements that lead to CO_2 bonding and activation. Sometimes the difficulty to extract general concepts derives from the fact that the results are obtained under different reaction conditions, on different surfaces, with different methods.

In this work we have performed a comparative study using exactly the same computational framework, DFT+U including dispersion contributions, of the bonding mechanism and degree of activation of CO_2 interacting with model catalysts consisting of single Cu atoms or Cu clusters supported on the rutile (110) and anatase (101) surfaces. Considering an isolated Cu atom and a Cu nanocluster allows us to compare two systems without and with metal-metal bonds, respectively, in the very same process. At the same time, oxygen vacancies have been created on the oxide support, in order to identify the importance that these defects have on the reaction. The level of CO_2 activation has been monitored by analyzing the distortion occurring upon adsorption and the strength of the surface chemical bond.

The results can be summarized in the following points:

- CO_2 activation on Cu/TiO_2 single atoms and Cu nanoclusters is surface sensitive, as the rutile and anatase surfaces can exhibit different behaviors mainly related to the different morphology of the two surfaces.
- The atomic structure of the oxide surface is essential since CO_2 is activated only when the molecule can simultaneously bind to at least two active sites, such as a Cu atom on one side and a Ti ion on the other site. The presence of at least two binding sites is essential for CO_2 activation, and this is also the main message of the paper.
- Single Cu atoms bound on TiO_2 become positively charged (+I oxidation state) due to a spontaneous electron transfer to both rutile and anatase supports; the Cu single atoms can bind and activate CO_2 at variance with the bare surfaces, facilitating a charge transfer from the oxide to the adsorbed CO_2 molecule.
- Small Cu clusters can bind and activate CO_2 thanks to the special reactivity of the Cu, O and Ti atoms at the metal/oxide interface showing the important role of this region for the activity of supported metal particles.
- Oxide reduction can have an important role provided that the oxygen vacancies are in direct contact with the Cu catalyst. The presence of O vacancy sites facilitates the spontaneous dissociation of CO_2 to CO, or it increases the electron density of the metal catalyst resulting in higher activity. The first process can drive CO_2 to methanol conversion following the so-called reverse water gas-shift reaction; the second case can facilitate CO_2 to methanol conversion via formate mechanism.

Computational Details

Spin polarized DFT calculations have been performed with the Vienna Ab Initio Simulation Package (VASP 5.4.4)[50–52] code using the generalized gradient approximation of the exchange and correlation functional with the Perdew-Burke-Ernzerhof (PBE)[53] formalism. The PBE+U approach[54,55] has been adopted with the purpose to partially correct the self-interaction error.[54,56] Here, the Hubbard parameter for the d-orbitals of Ti was set as U−J = 3 eV.[57] Dispersion forces were included considering the Grimme's D3 parametrization.[58] The valence electrons considered explicitly were C (2s, 2p), O (2s, 2p), Ti (3s, 4s, 3p, 3d) and Cu (4s, 3d); they were expanded by a set of plane waves with a kinetic energy cutoff of 400 eV. The core electrons were treated with pseudo-potentials considering the projector augmented wave approach (PAW).[59,60] Regarding electronic and ionic loops, the threshold criteria were set at 10^{-5} eV and 10^{-2} eV/Å, respectively. For Brillouin-zone integration, a 1×1×1 Monkhorst–Pack k-point grid[61] was used.

A 3×1 supercell of anatase (101) and two 3×2 and 3×3 supercells of rutile (110) were created using the optimized TiO_2 bulk lattice parameters. The atomic positions of the supercell were then fully optimized and a vacuum > 10 Å was added to avoid the interaction between periodic replicas. The obtained lattice parameters are: a = 11.381 Å, b = 10.389 Å and $\gamma = 90°$ for anatase and a = 8.973 Å, b = 13.104 Å and $\gamma = 90°$ for rutile.

On these structures, a Cu atom and a Cu_{10} cluster were adsorbed, and the energy of adsorption (E_{ads}) was calculated according to the following equation [Eq. (1)]:

$$E_{ads} = E(Cu_x/TiO_2) - E(TiO_2) - E(Cu_x) \quad (1)$$

where $E(Cu_x/TiO_2)$ is the energy of the combined system and $E(TiO_2)$ and $E(Cu_x)$ the energies of isolated species.

O vacancies were created by removing one oxygen atom from various sites, and the vacancy formation energy (E_f) was calculated according to the following equation [Eq. (2)]:

$$E_f = E(TiO_{2-x}) + E(O_2)/2 - E(TiO_2) \quad (2)$$

where $E(TiO_{2-x})$ is the energy of the final system with the O vacancy, $E(O_2)$ the energy of the oxygen molecule and $E(TiO_2)$ the energy of the initial stoichiometric system.

CO_2 and CO molecules were adsorbed on the different systems and their adsorption energies were calculated as the difference between the energy of the final structures (E_{final}) and the energies of catalyst (E_{cat}) and the molecules (E_{mol}) in the gas phase [Eq. (3)]:

$$E_{ads} = E_{final} - (E_{cat} + E_{mol}) \quad (3)$$

Acknowledgements

We acknowledge the financial support from CARIPLO Foundation, project ''Carbon dioxide conversion into energy-rich molecules with tailored catalysts''. This research was funded by the European Union – NextGenerationEU, Italian National Recovery and Resilience Plan, Mission 4, Component 2, Investment 1.5 "Innovation Ecosystems", project MUSA". Access to the CINECA supercomputing resources was granted via ISCRAB. Open Access funding provided by Università degli Studi di Milano-Bicocca within the CRUI-CARE Agreement.

Conflict of Interests

The authors declare no conflict of interest.

Data Availability Statement

All inputs and outputs of the DFT calculations of the complexes reported in the paper are available upon reasonable request to the authors.

Keywords: CO_2 activation · DFT calculations · single atom catalyst · supported cluster · TiO_2

[1] I. Sullivan, A. Goryachev, I. A. Digdaya, X. Li, H. A. Atwater, D. A. Vermaas, C. Xiang, *Nat. Catal.* **2021**, *4*, 952–958.
[2] C. A. Trickett, A. Helal, B. A. Al-Maythalony, Z. H. Yamani, K. E. Cordova, O. M. Yaghi, *Nat. Rev. Mater.* **2017**, *2*, 17045.
[3] Y. Wang, E. Chen, J. Tang, *ACS Catal.* **2022**, *12*, 7300–7316.
[4] M. Favaro, H. Xiao, T. Cheng, W. A. Goddard, J. Yano, E. J. Crumlin, *Proc. Nat. Acad. Sci.* **2017**, *114*, 6706–6711.
[5] E. L. Kunkes, F. Studt, F. Abild-Pedersen, R. Schlögl, M. Behrens, *J. Catal.* **2015**, *328*, 43–48.
[6] T. Reichenbach, K. Mondal, M. Jäger, T. Vent-Schmidt, D. Himmel, V. Dybbert, A. Bruix, I. Krossing, M. Walter, M. Moseler, *J. Catal.* **2018**, *360*, 168–174.
[7] M. Luo, Z. Wang, Y. C. Li, J. Li, F. Li, Y. Lum, D.-H. Nam, B. Chen, J. Wicks, A. Xu, T. Zhuang, W. R. Leow, X. Wang, C.-T. Dinh, Y. Wang, Y. Wang, D. Sinton, E. H. Sargent, *Nat. Commun.* **2019**, *10*, 5814.
[8] P.-P. Yang, X.-L. Zhang, F.-Y. Gao, Y.-R. Zheng, Z.-Z. Niu, X. Yu, R. Liu, Z.-Z. Wu, S. Qin, L.-P. Chi, Y. Duan, T. Ma, X.-S. Zheng, J.-F. Zhu, H.-J. Wang, M.-R. Gao, S.-H. Yu, *J. Am. Chem. Soc.* **2020**, *142*, 6400–6408.
[9] C. Chen, X. Yan, S. Liu, Y. Wu, Q. Wan, X. Sun, Q. Zhu, H. Liu, J. Ma, L. Zheng, H. Wu, B. Han, *Angew. Chem.* **2020**, *100049*, 16601–16606.
[10] T. Lunkenbein, J. Schumann, M. Behrens, R. Schlögl, M. G. Willinger, *Angew. Chem.* **2015**, *127*, 4627–4631; *Angew. Chem. Int. Ed.* **2015**, *54*, 4544–4548.
[11] L. Liu, A. Corma, *Nat. Rev. Mater.* **2021**, *6*, 244–263.
[12] S. Mitchell, J. Pérez-Ramírez, *Nat. Rev. Mater.* **2021**, *6*, 969–985.
[13] X. Deraet, J. Turek, M. Alonso, F. Tielens, B. M. Weckhuysen, M. Calatayud, F. De Proft, *ChemPhysChem* **2023**, *24*, e202200785.
[14] S. K. Sharma, A. Banerjee, B. Paul, M. K. Poddar, T. Sasaki, C. Samanta, R. Bal, *J. CO2 Util.* **2021**, *50*, 101576.
[15] A. R. Haines, J. C. Hemminger, *ACS Catal.* **2021**, *11*, 6960–6970.
[16] C. Liu, S. L. Nauert, M. A. Alsina, D. Wang, A. Grant, K. He, E. Weitz, M. Nolan, K. A. Gray, J. M. Notestein, *Appl. Catal. B* **2019**, *255*, 117754.
[17] D. Liu, Y. Fernández, O. Ola, S. Mackintosh, M. Maroto-Valer, C. M. A. Parlett, A. F. Lee, J. C. S. Wu, *Catal. Commun.* **2012**, *25*, 78–82.
[18] G. Pacchioni, *ChemPhysChem* **2003**, *4*, 1041–1047.
[19] L. DeRita, J. Resasco, S. Dai, A. Boubnov, H. V. Thang, A. S. Hoffman, I. Ro, G. W. Graham, S. R. Bare, G. Pacchioni, X. Pan, P. Christopher, *Nat. Mater.* **2019**, *18*, 746–751.
[20] H. V. Thang, G. Pacchioni, L. DeRita, P. Christopher, *J. Catal.* **2018**, *367*, 104–114.
[21] C. Asokan, H. V. Thang, G. Pacchioni, P. Christopher, *Catal. Sci. Technol.* **2020**, *10*, 1597–1601.
[22] L. Zhang, H. Bi, Z. Wang, G. Zhou, *Int. J. Hydrogen Energy* **2022**, *47*, 4653–4661.
[23] S.-F. Peng, J.-J. Ho, *Phys. Chem. Chem. Phys.* **2011**, *13*, 20393.
[24] T. Wang, S. Qiu, Z. Dai, R. Hocking, C. Sun, *Appl. Surf. Sci.* **2020**, *533*, 147362.
[25] F. Kraushofer, G. S. Parkinson, *Chem. Rev.* **2022**, *122*, 14911–14939.
[26] C. Franchini, M. Reticcioli, M. Setvin, U. Diebold, *Nat. Rev. Mater.* **2021**, *6*, 560–586.
[27] E. Finazzi, C. Di Valentin, G. Pacchioni, A. Selloni, *J. Chem. Phys.* **2008**, *129*, 154113.
[28] P. Schlexer, H.-Y. T. Chen, G. Pacchioni, *Catal. Lett.* **2017**, *147*, 1871–1881.
[29] C. Di Valentin, G. Pacchioni, A. Selloni, *Phys. Rev. Lett.* **2006**, *97*, 166803.
[30] Y. Zhang, Y. Wang, K. Su, F. Wang, *J. Mol. Model.* **2022**, *28*, 175.
[31] M. V. Ganduglia-Pirovano, A. Hofmann, J. Sauer, *Surf. Sci. Rep.* **2007**, *62*, 219–270.
[32] H. Cheng, A. Selloni, *Phys. Rev. B* **2009**, *79*, 92101.
[33] M. Setvín, U. Aschauer, P. Scheiber, Y.-F. Li, W. Hou, M. Schmid, A. Selloni, U. Diebold, *Science* **2013**, *341*, 988–991.
[34] G. Pacchioni, H. Freund, *Chem. Rev.* **2013**, *113*, 4035–4072.
[35] H. V. Thang, G. Pacchioni, *J. Phys. Chem. C* **2019**, *123*, 7271–7282.
[36] K. I. Hadjiivanov, G. N. B. T.-A. in C. Vayssilov, Academic Press, **2002**, pp. 307–511.
[37] G. Pacchioni, G. Cogliandro, P. S. Bagus, *Surf. Sci.* **1991**, *255*, 344–354.
[38] U. Diebold, *Surf. Sci. Rep.* **2003**, *48*, 53–229.
[39] D. C. Sorescu, J. Lee, W. A. Al-Saidi, K. D. Jordan, *J. Chem. Phys.* **2011**, *134*, 104707.
[40] L. Mino, G. Spoto, A. M. Ferrari, *J. Phys. Chem. C* **2014**, *118*, 25016–25026.
[41] P. Schlexer, H.-Y. T. Chen, G. Pacchioni, *Catal. Lett.* **2017**, *147*, 1871–1881.
[42] F. Viñes, J. R. B. Gomes, F. Illas, *Chem. Soc. Rev.* **2014**, *43*, 4922–4939.
[43] P. Schlexer, D. Widmann, R. J. Behm, G. Pacchioni, *ACS Catal.* **2018**, *8*, 6513–6525.
[44] D. Widmann, R. J. Behm, *Acc. Chem. Res.* **2014**, *47*, 740–749.
[45] M. Qiu, Z. Fang, Y. Li, J. Zhu, X. Huang, K. Ding, W. Chen, Y. Zhang, *Appl. Surf. Sci.* **2015**, *353*, 902–912.
[46] S. Kattel, P. J. Ramírez, J. G. Chen, J. A. Rodriguez, P. Liu, *Science* **2017**, *355*, 1296–1299.
[47] A. Ruiz Puigdollers, P. Schlexer, S. Tosoni, G. Pacchioni, *ACS Catal.* **2017**, *7*, 6493–6513.
[48] L. G. Dodson, M. C. Thompson, J. M. Weber, *Annu. Rev. Phys. Chem.* **2018**, *69*, 231–252.
[49] D. Goud, R. Gupta, R. Maligal-Ganesh, S. C. Peter, *ACS Catal.* **2020**, *10*, 14258–14282.
[50] G. Kresse, J. Hafner, *Phys. Rev. B* **1993**, *47*, 558–561.
[51] G. Kresse, J. Hafner, *Phys. Rev. B* **1994**, *49*, 14251–14269.
[52] G. Kresse, J. Furthmüller, *Comput. Mater. Sci.* **1996**, *6*, 15–50.
[53] J. P. Perdew, K. Burke, M. Ernzerhof, *Phys. Rev. Lett.* **1996**, *77*, 3865–3868.
[54] S. L. Dudarev, G. A. Botton, S. Y. Savrasov, C. J. Humphreys, A. P. Sutton, *Phys. Rev. B* **1998**, *57*, 1505–1509.
[55] A. I. Liechtenstein, V. I. Anisimov, J. Zaanen, *Phys. Rev. B* **1995**, *52*, R5467-R5470.
[56] V. I. Anisimov, J. Zaanen, O. K. Andersen, *Phys. Rev. B* **1991**, *44*, 943–954.
[57] S. Tosoni, H.-Y. T. Chen, A. Ruiz Puigdollers, G. Pacchioni, *Philos. Trans. R. Soc. London* **2017**, *376*, 20170056.
[58] S. Grimme, J. Antony, S. Ehrlich, H. Krieg, *J. Chem. Phys.* **2010**, *132*, 10.1063/1.3382344.
[59] P. E. Blöchl, *Phys. Rev. B* **1994**, *50*, 17953–17979.
[60] G. Kresse, D. Joubert, *Phys. Rev. B* **1999**, *59*, 1758–1775.
[61] H. J. Monkhorst, J. D. Pack, *Phys. Rev. B* **1976**, *13*, 5188–5192.

Manuscript received: March 8, 2023
Accepted manuscript online: April 6, 2023
Version of record online: May 4, 2023